

The use of Acoustic Emission for bearing defect identification and estimation of defect size

Abdullah M. Al-Ghamdi¹, D. Zhechkov and D. Mba²

¹Mechanical Services Shops Department, Saudi Aramco, Dhahran, Saudi Arabia
Tel: +966 (0) 3-872-3270, Fax: +966 (0) 3-872-0571, abdullah.ghamdi.52@aramco.com

²School of Engineering, Cranfield University, Bedfordshire. MK43 0AL, UK
Tel: +44 (0) 1234-754681, Fax: +44 (0) 1234-751566, d.mba@cranfield.ac.uk

Abstract

Vibration monitoring of rolling element bearings is possibly the most established diagnostic technique for rotating machinery. The application of Acoustic Emission (AE) for bearing diagnosis is gaining ground as a complementary diagnostic tool; however, limitations in the successful application of the AE technique have been partly due to the difficulty in processing, interpreting and classifying the acquired data. Furthermore, the extent of bearing damage from the defect has eluded the AE diagnostician. The investigation reported in this paper was centered on the application of the Acoustic Emission technique for identifying the presence and size of a defect on a radially loaded bearing. An experimental test-rig was designed such that defects of varying sizes could be seeded onto the outer race of a test bearing. Comparisons between AE and vibration analysis, over a range of speed and load conditions, are presented. It is concluded that not only does AE offer earlier fault detection and identification capabilities than vibration analysis but can also provide an indication of the defect size, thus allowing the user to monitor the rate of degradation on the bearing.

Introduction

Acoustic emissions (AE) are defined as transient elastic waves generated from a rapid release of strain energy caused by a deformation or damage within or on the surface of a material [1]. In this particular investigation, AE's are defined as the transient elastic waves generated by the interaction of two surfaces in relative motion. The interaction of surface asperities and impingement of the bearing rollers over the seeded defect on the outer race will generate AE's. Due to the high frequency content of the AE signatures typical mechanical noise (less than 20KHz) is eliminated, as are other low frequency mechanical defects such as imbalance, misalignment and shaft bending. Roger [2] utilised the AE technique for monitoring slow rotating anti-friction slew bearings on cranes employed for gas production. In addition, successful applications of AE to bearing diagnosis for extremely slow rotational speeds have been reported [3, 4]. Yoshioka and Fujiwara [5, 6] have shown that selected AE parameters identified bearing defects before they appeared in the vibration acceleration range. Hawman et al [7] reinforced Yoshioka's observation and noted that diagnosis of defect bearings was accomplished due to modulation of high frequency AE bursts at the outer race defect frequency. The modulation of AE signatures at bearing defect frequencies has also been observed by other researchers [8, 9, 10]. Morhain et al [11] showed successful application of AE to monitoring split bearings.

This paper investigates the relationship between AE r.m.s, amplitude and kurtosis for a range of defect conditions, offering a more comprehensive study than is presently available in the public domain. Moreover, comparisons with vibration analysis are presented. The source of AE is investigated, the results of which conclusively identify the dominant AE source mechanism for bearing defect conditions. Finally a relationship between AE burst duration and defect size is presented, the first known detailed attempt.

Experimental Test Rig and Test Bearing

The bearing test rig employed for this study had an operational speed range of 10 to 4000 rpm with a maximum load capability of 16 kN via a hydraulic ram. The test bearing employed was a Cooper split type roller bearing (01B40MEX). The split type bearing was selected as it allowed defects to be seeded onto the races, furthermore, assembly and disassembly of the bearing was accomplished with minimum disruption to the test sequence see figure 1. Characteristics of the test bearing (Split Cooper, type 01C/40GR) were: Internal (bore) diameter, 40mm; External diameter, 84mm; Diameter of roller, 12mm; Diameter of roller centers, 166mm; Number of rollers, 10. Based on these geometric properties the outer race defect frequency was determined at '4.1X' (4.1 times the rotation shaft speed).

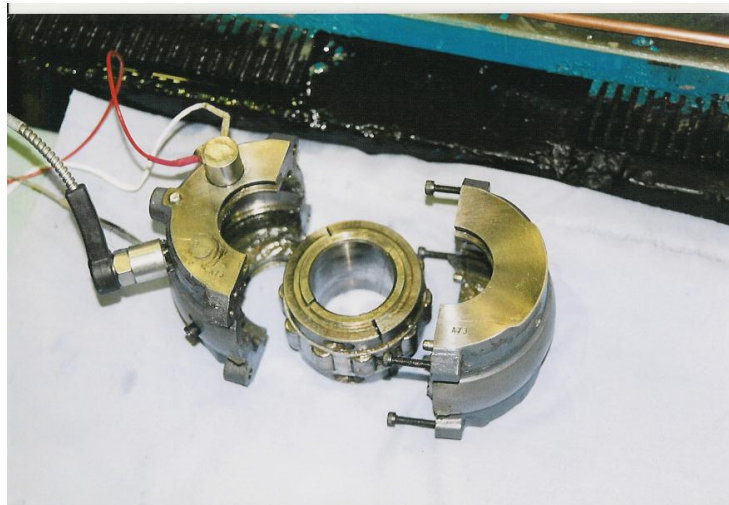


Figure 1 **Test bearing**

Data Acquisition System

The transducers employed for vibration and AE data acquisition were placed directly on the bearing housing of the bearing, see figure 1. A piezoelectric type AE sensor (Physical Acoustic Corporation type WD) with an operating frequency range of 100 kHz – 1000 kHz was employed whilst a resonant type accelerometer, with a flat frequency response between 10 Hz and 8000 Hz (Model 236 Isobase accelerometer, 'Endevco Dynamic Instrument Division') was used for vibration measurement. Pre-amplification was set at 40dB. A total of 256,000 data points were recorded per acquisition (data file) at a sampling rate of 2MHz. Twenty (20) data files were recorded for each simulated case, see experimental procedure. The acquisition of vibration data was sampled at 2.5kHz for a total of 12,500 data points.

Signal processing

Whilst numerous signal processing are applicable for the analysis of acquired data, the author's have opted for simplicity in diagnosis, particularly if this technique is to be readily adopted by industry. The AE parameters measured for diagnosis in this particular investigation were amplitude and r.m.s. These were compared with corresponding parameters from vibration data. It is worth stating that the selected parameters are typical for vibration analysis.

Experimental procedure

Two test programmes were undertaken. Firstly, a research investigation to ascertain the primary source of AE activity from seeded defects on bearings was undertaken, in addition to determining the relationship between defect size, AE and vibration activity. In an attempt to identify the primary source of AE activity a surface topography of the various defects were taken. Furthermore, two types of defect conditions were simulated; firstly, a surface discontinuity that did not result in a protrusion above the average surface roughness of the race. The second defect type resulted in protrusions that were clearly above the surface roughness. The second test programme aimed to establish a correlation between AE activities for controlled incremental defect sizes at a fixed speed. Prior to defect simulations for all test programmes baseline, or defect free, recordings were undertaken for twelve running conditions; four speed (600, 1000, 20000 and 3,000 rpm) and three load conditions (0, 4.43kN and 8.86kN). Defects were simulated with the use of an engraving machining employing a carbide tip.

Test programme 1; Defects of different severities

For these tests five defect test conditions were simulated with varying severities on the outer race of the test bearing. The simulations were; defect free condition, a point defect engraved onto the outer race which was approximately 0.85 x 0.85mm, a line defect, approximately 5.6 x 1.2 mm, see figures 2 and 4, a rough defect, approximately 17.5 x 9.0 mm, and a smooth defect in which a surface discontinuity, not influencing the average surface roughness, was simulated. In this particular instance a grease hole matched the requirements, see figures 3 and 5. From figure 5 it is evident that the point of discontinuity of the surface does not have material protrusions as evident for the 'point' or 'line' defect conditions, see figure 4. The main purpose of this simulation is to observe if any changes in the load distribution will lead to generation or changes in AE activity in comparison to a continuous surface, 'defect free' condition. All defects are run under four speeds (600, 1000, 2000 and 3000 rpm) and three different loads (0, 4.43 and 8.86 kN).

Test programme 2; Defects of different severities

For this particular simulation a point defect was increased in size in seven incremental steps. The increase in length is detailed in table 1. All of these defects are run at 2000 rpm and under two load conditions (4.43 kN [load 1] and 8.86 kN [load 2]). For these particular tests a sampling rate of 10MHz was employed.



Figure 2 Line defect simulation

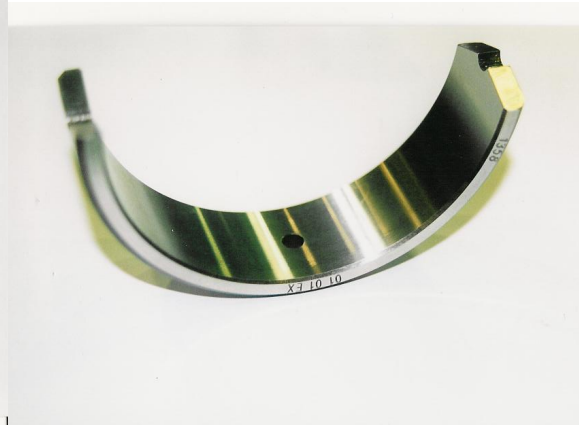


Figure 3 Smooth defect condition

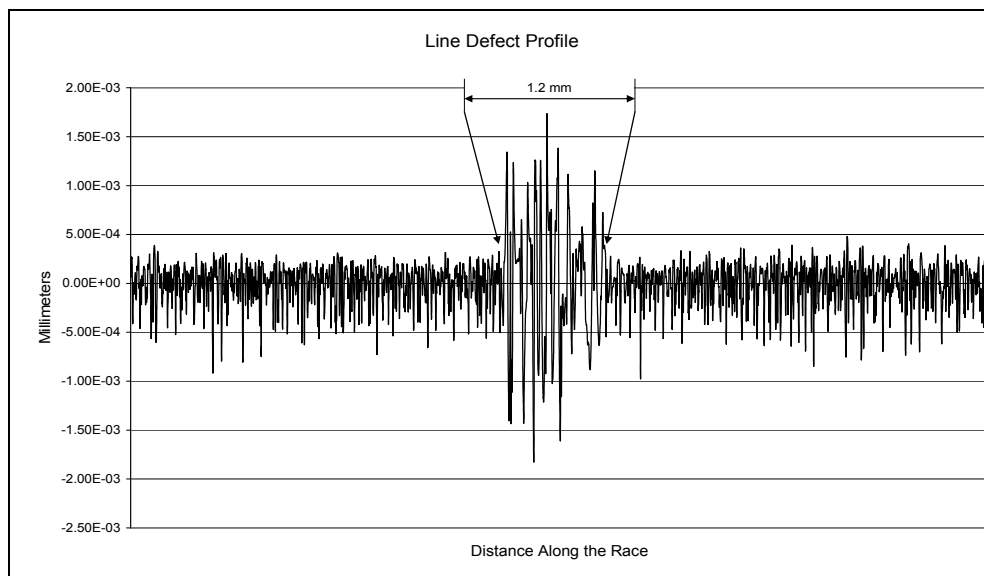


Figure 4 Surface profile of a line defect condition showing material protrusion above average surface roughness

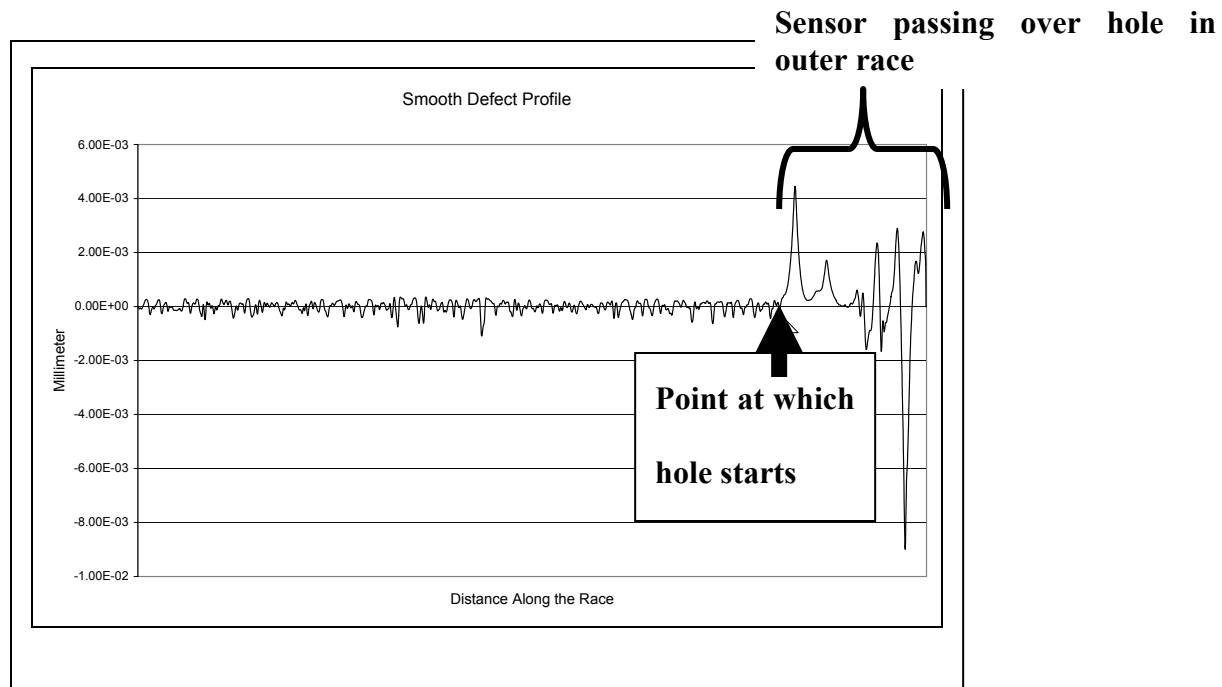


Figure 5 Surface profile of a smooth defect condition showing NO material protrusion above average surface roughness

Analysis Procedure

If the defects simulated were to produce AE transients, as each rolling element passed the defect, it was envisaged that the AE bursts would be detected at a rate equivalent to the outer race defect frequency ('4.1X'). In addition, it was also anticipated that the defect frequency would be observed in the vibration frequency range. Furthermore, the AE and vibration r.m.s and maximum amplitude values were calculated. Approximately twenty AE data files were captured per fault simulated. This was equivalent to one, two, four and six revolutions at speeds of 600, 1000, 2000 and 3000 rpm respectively. Every data file was broken into sections equivalent to one revolution. The diagnostic parameters r.m.s, etc, were calculated for each shaft revolution and averaged for all data files. For example this was equivalent to averaging over twenty revolutions at 1000rpm. For vibration analysis, two data files were acquired for each simulation. This was equivalent to 50, 83, 166 and 250 revolutions per data file at speeds of 600, 1000, 2000 and 3000 rpm respectively. The exact procedure for calculating the AE parameters was employed on the vibration data

Time domain AE observations

As already stated the outer race defect frequency was calculated for the various test speeds; 41, 69, 137 and 205 Hz at 600, 1000, 2000 and 3000rpm respectively. Typical AE waveform for a defect condition is displayed in figure 6. It was noted that for all defects conditions, other than the smooth defect, AE burst activity was noted at the outer race defect frequency, a typical example is shown in figure 6. Observations of AE time waveforms for the noise and smooth defect conditions showed random AE bursts that occurred at a rate which could not be related to any machine cyclic phenomenon. Correspondingly, such transient bursts were not observed on vibration waveforms, but more interestingly, the outer race defect frequency was not observed on

the frequency spectra of most vibration data, except at one defect condition; rough defect, 3000rpm, load 0kN.

Table 1 Notation for testing and labelling data

		Defect Type (W x L)		Speed (rpm)		Load (kN)	
Defects of Different Severities	N	Noise (No Defect)	S1	600	L0	0	
	SD	Smooth Defect	S2	1000	L1	4.43	
	PD	Point Defect 0.85x0.85 mm	S3	2000	L2	8.86	
	LD	Line Defect 5.6x1.2 mm	S4	3000			
	RD	Big Rough Defect 17.5x9.0 mm					
Defects of Different Sizes	D1	0.85 x 1.35 mm	D2	2. x 1.35 mm	D3	2 x 4 mm	
	D4	4 x 4 mm	D5	8 x 4 mm	D6	13 x 4 mm	
	D7	13x 10 mm					
Second Type of tests							

Observations of r.m.s and maximum amplitude values

The r.m.s values of AE and vibration signatures for all defect and defect free conditions were compared for increasing speeds and increasing loads, see figures 7 and 8. For all test conditions, the AE r.m.s value increased with increasing speed and load. It was also noted that the AE r.m.s values of noise and smooth defect were similar while AE r.m.s values increased with increased defect severity; point, line and rough defects respectively. Vibration r.m.s values for all the point and line defect, and, noise and smooth defect condition, were very similar, however, a clear increase in vibration r.m.s was observed for the rough defect, see figure 8.

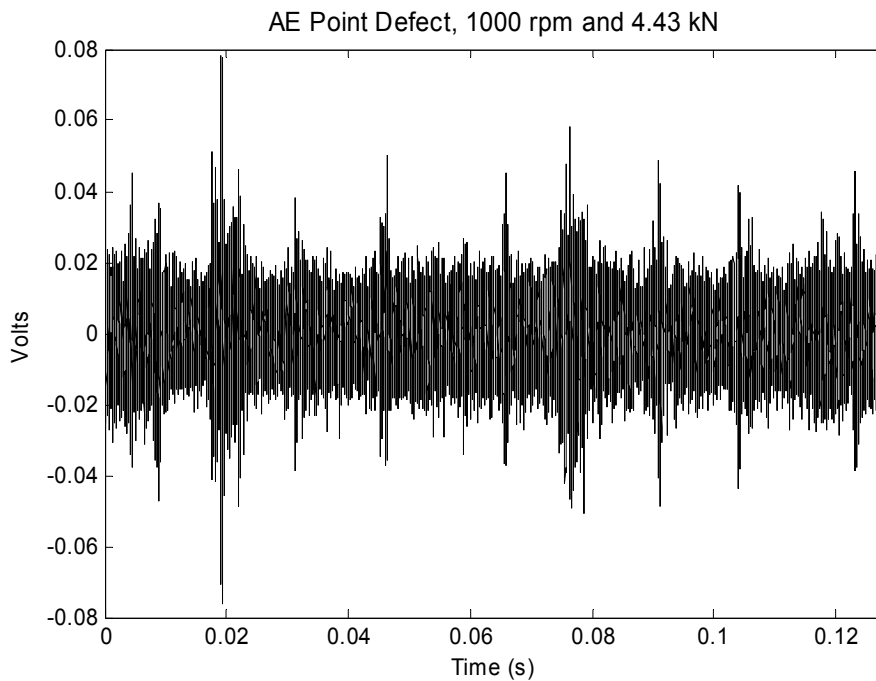


Figure 6 AE time waveform 'Point defect'; Speed (1000 rpm), Load (4.43 kN)

It was noted that AE max amplitude increased with increasing speed for a fixed load. Also it was evident that as the defect size was increased, the maximum AE amplitude increased. The maximum AE amplitude increased from noise condition to the point defect and increased further for the line defect. Observations of the change of AE r.m.s and maximum amplitude values for different defect sizes, emphasised the sensitivity of AE to defect size progression.

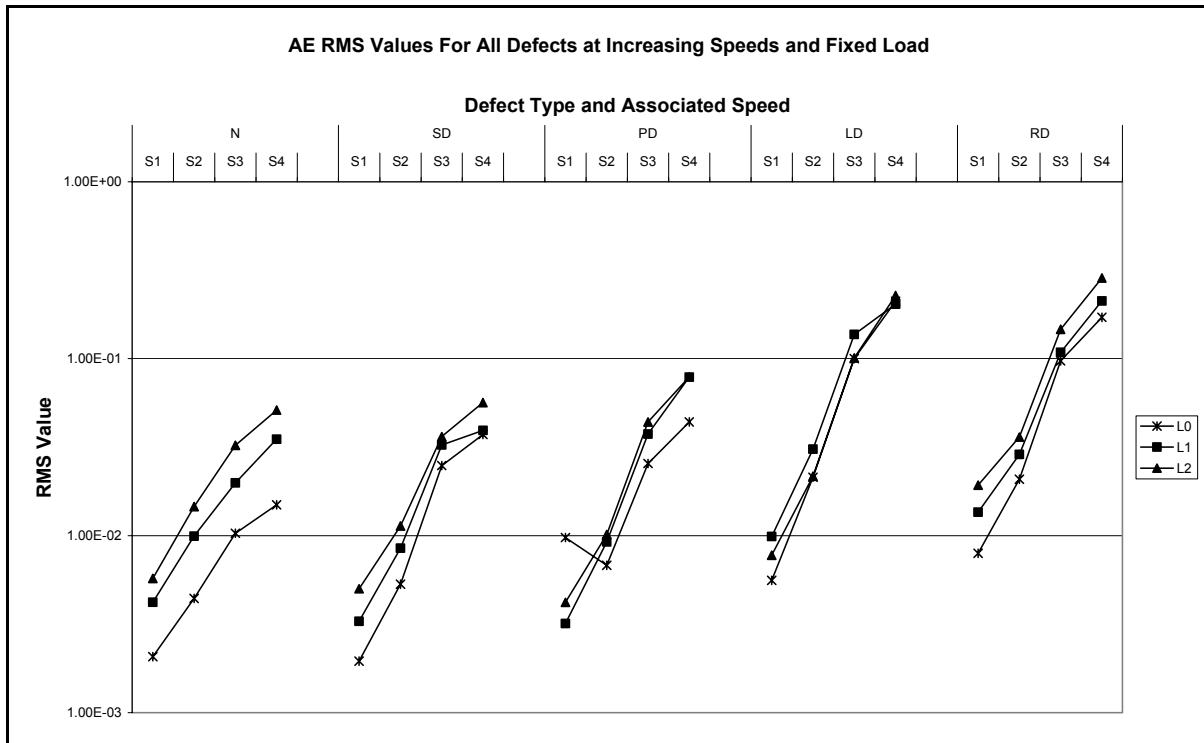


Figure 7 AE r.m.s observations for all test conditions

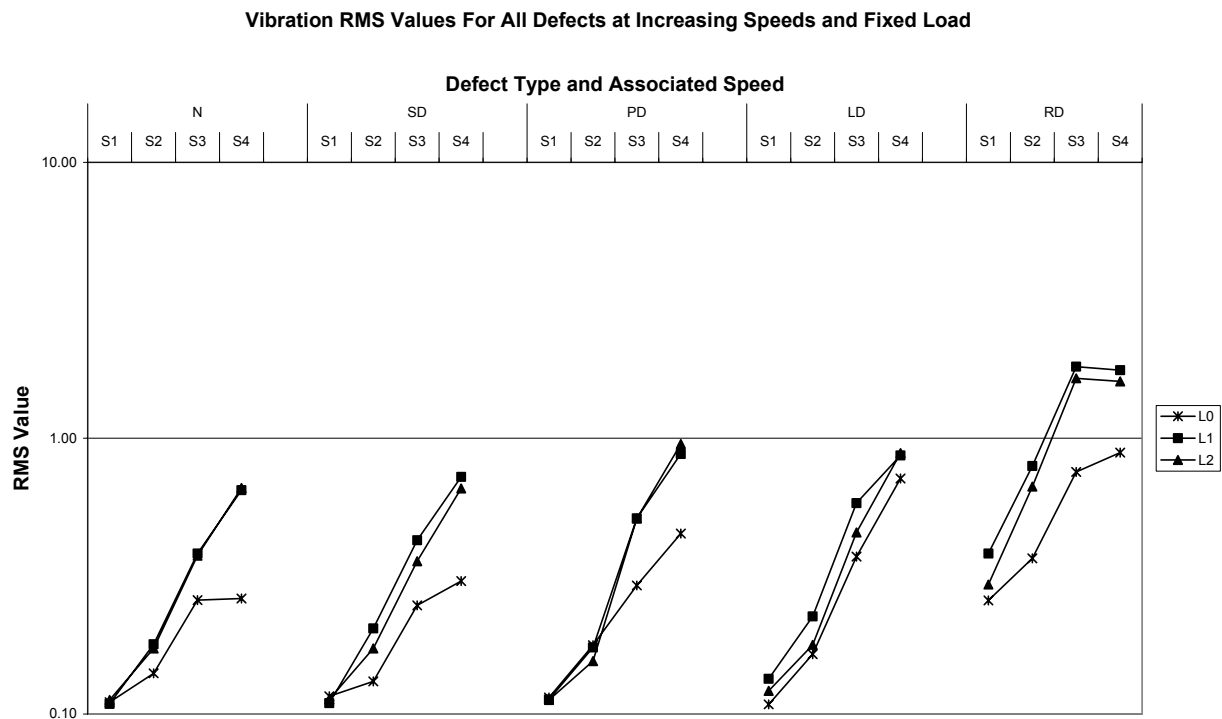


Figure 8 Vibration r.m.s observations for all test conditions

Defect size observations

Observations of the AE time waveform showed that the duration of the transient AE bursts associated with the defect increased with increasing defect size, particularly from defect size D3 to D7, see figures 9 and 10. Clearly this showed that AE burst duration might hold information to indicate the size of defect.

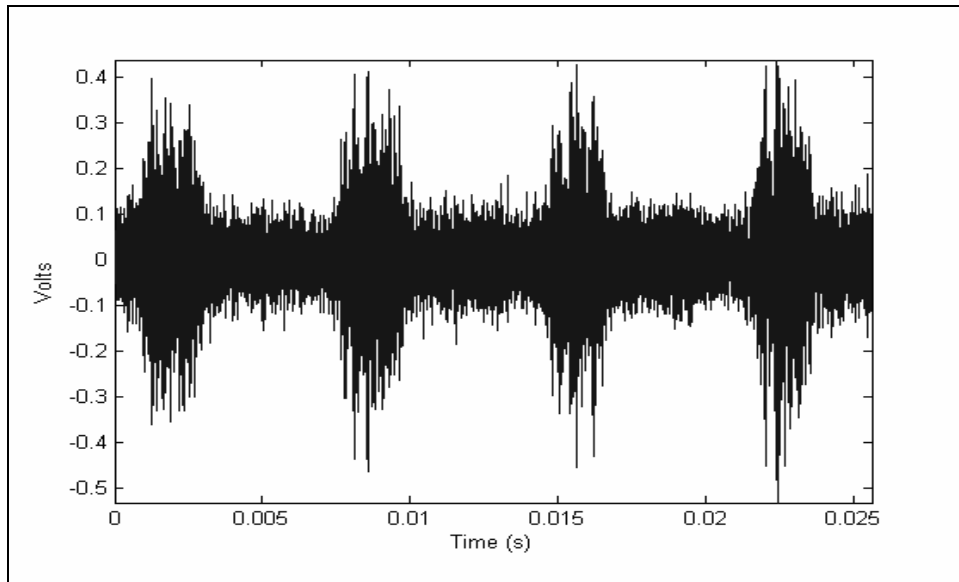


Figure 9 AE waveform for defect size D6 highlight the duration of the AE transient bursts associated with the outer race defect (sampling rate 10MHz).

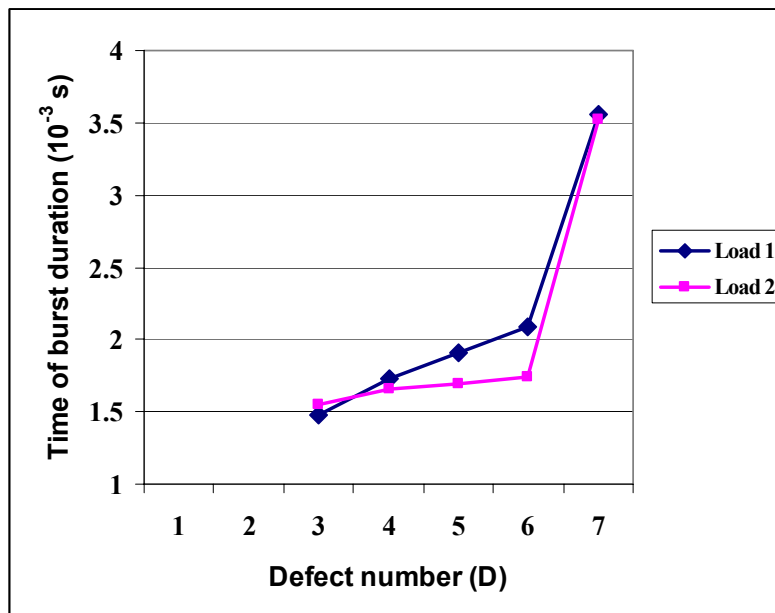


Figure 10 AE burst duration as a function of defect size (D)

Conclusions

It has been shown that the fundamental source of AE in bearings is due to material protrusions above the mean surface roughness. This causes impacting as the rollers pass over thereby generating AE activity. It has also been shown that analysis of AE r.m.s and maximum amplitude is more sensitive to defect identification than vibration analysis, moreover, AE offers the potential to ascertain the defect size by observations of the associated AE burst duration.

References

- 1 Mathews, J. R. *Acoustic emission*, Gordon and Breach Science Publishers Inc., New York. 1983, ISSN 0730-7152.
- 2 Roger, L. M., The application of vibration analysis and acoustic emission source location to on-line condition monitoring of anti-friction bearings. *Tribology International*, 1979; 51-59.
- 3 Mba, D., Bannister, R.H., and Findlay, G.E. Condition monitoring of low-speed rotating machinery using stress waves: Part's I and II. *Proceedings of the Instn Mech Engr* 1999; 213(E): 153-185.
- 4 N. Jamaludin, Dr. D. Mba, Dr. R. H. Bannister Condition monitoring of slow-speed rolling element bearings using stress waves. *Journal of Process Mechanical Engineering*, I Mech E. Pro. Inst. Mech Eng., 2001, 215(E);, Issue E4, 245-271.
- 5 Yoshioka T, Fujiwara T. New acoustic emission source locating system for the study of rolling contact fatigue, *Wear*, 81(1), 183-186.
- 6 Yoshioka T, Fujiwara T. Application of acoustic emission technique to detection of rolling bearing failure, *American Society of Mechanical Engineers*, Production Engineering Division publication PED, 1984, 14, 55-76.
- 7 Hawman, M. W., Galinaitis, W. S, Acoustic Emission monitoring of rolling element bearings, *Proceedings of the IEEE, Ultrasonics symposium*, 1988, 885-889.
- 8 Holroyd, T.J. and Randall, N., (1993), Use of Acoustic Emission for Machine Condition Monitoring, *British Journal of Non-Destructive Testing*, 1993, 35(2), 75-78.
- 9 Holroyd, T. Condition monitoring of very slowly rotating machinery using AE techniques. *14th International congress on Condition monitoring and Diagnostic engineering management (COMADEM'2001)*, Manchester, UK, 4-6 September 2001, 29, ISBN 0080440363
- 10 Bagnoli, S., Capitani, R. and Citti, P. Comparison of accelerometer and acoustic emission signals as diagnostic tools in assessing bearing. *Proceedings of 2nd International Conference on Condition Monitoring*, London, UK, May 1988, 117-125.
- 11 Morhain, A, Mba, D, Bearing defect diagnosis and acoustic emission *Journal of Engineering Tribology*, I Mech E, Vol 217, No. 4, Part J, p 257-272, 2003. ISSN 1350-6501.